



ELSEVIER

Measurement 24 (1998) 187–196

Measurement

Measurement of human baroreceptor reflex sensitivity by means of parametric identification

Mariolino De Cecco^{a,*}, Alessandro Angrilli^b

^a*Dipartimento di Meccanica, Facoltà di Ingegneria, via Venezia 1, 35131 Padova, Italy*

^b*Dipartimento di Psicologia Generale, Facoltà di Psicologia, via Venezia 8, 35131 Padova, Italy*

Received 15 December 1997; received in revised form 15 July 1998; accepted 9 August 1998

Abstract

The development of a technique for measuring the sensitivity of baroreceptors is described. This technique exploits the principles of parametric identification using ARMAX models: the input–output behaviour (systolic pressure–heart rate) of the baroreceptor system is identified, and thus its sensitivity. The cost function for choosing the model is defined by generalising the classic sum of square residuals, i.e., introducing cross-correlation between input and residuals and auto-correlation of residuals. The resulting algorithm is compared with the ‘modulus’ technique (Robbe et al., 1987) by means of simulated data with added noise. In the case of modulus, the systematic error increases considerably with noise. This tendency towards overestimation is quantified to +18% (percentage error divided by ratio of noise to signal root-mean-square values), whereas that of the proposed technique is only +2.5%. Experimental data was used to study the correlation between the measurements obtained using the two techniques (Pearson’s correlation index was 0.81). This analysis confirmed the tendency to overestimation of modulus. © 1998 Elsevier Science Ltd. All rights reserved.

Keywords: Baroreceptor; Parametric Identification; Blood Pressure

1. Introduction

Baroreceptors are mechanoreceptors located in the aortic arch and carotid sinus, and sensitive to the mechanical stretch of the arterial wall. When the arterial diameter increases, following an increase in blood pressure, the baroreceptors increase their firing rate.

The negative feedback represented by the baroreceptor reflex is homeostatic control of blood pressure. When blood pressure increases, the baroreceptors increase their firing rate and this causes a

decrease in blood pressure and heart rate. The reverse effect is observed when blood pressure decreases.

Medical research has recently focused greater attention on the baroreceptor reflex, because its alteration seems to be involved in hypertension [1]. The risk of hypertension development may be evaluated by means of baroreceptor reflex sensitivity [2–4]. This parameter has also prognostic importance for myocardial infarction [5].

Several methods have been developed to measure baroreceptor sensitivity. It is measured in ms/mmHg (i.e., the change in successive R-wave intervals measured in ms induced by a change in systolic blood pressure measured in mmHg). The pharmaco-

*Corresponding author. Tel.: +39-49-827-6795; Fax: +39-49-827-6785; E-mail: dececco@mail.dim.unipd.it

logical method consists of phenylephrine bolus injection [6,7] which increases systolic blood pressure. Both pressure and heart-period changes, which are due to baroreceptor reflex, are measured and the ratio between the two variations computed. This method is intrinsically invasive and dangerous (especially when used on hypertensive subjects).

Of the non-invasive methods, one of the first reported in the literature was based on sequence analysis. The method calculates the mean slope between variations of heart period and blood pressure that naturally occur and which are in phase [4,8]. Its drawback is that it also analyses the non-correlated sequences that occur randomly. Spectral analysis techniques have also been applied to epochs of heart rate and systolic blood pressure in order to quantify baroreceptor gain [9]. The baroreceptor reflex gain computed in this way is called “modulus”. This technique exploits the function of spectral coherence to distinguish between spurious effects and input ones. Similarly, other authors have introduced an alpha coefficient to describe baroreceptor gain [7,10].

More recently, other methods based on parametric identification have been devised [7,11]. These techniques estimate open-loop baroreceptor sensitivity during closed-loop conditions, that is, under spontaneous variability of both heart period and blood pressure. According to some authors [12], autoregressive (identification) methods are suitable when compared to spectral methods; however, to our knowledge, no quantitative demonstration of such a difference has been provided.

The algorithm described here uses the ARMAX method to identify the input (systolic pressure) and output (heart rate) behaviour of the baroreceptor reflex, without considering the influence of respiration which was taken into account in [11]. In fact, respiration measurement introduces a further factor of uncertainty: finger blood pressure measurement does not provide good accuracy in the respiration band, because the coherence between non-invasive and invasive measures is lower in the 0.15–0.35 Hz frequency range [8]. This fact reduces the reliability of more complex models. Using the ARMAX model, the influence of respiration and of other effects (see par. 2) is taken into account as part of noise dynamics. As a further consideration, in the com-

parison between autoregressive methods, the Least Square Method (LSM) used in previous studies [7,11] is more sensitive to noise influence than the Prediction Error Method (PEM) used in the ARMAX estimation (noise is modelled and thus decoupled from measured signals [13]).

The proposed technique was correlated with the modulus method by means of data collected over a set of 23 subjects. Results are given in Section 5 together with noise sensitivity. The ability of ARMAX to model noise dynamics allows better precision in estimated sensitivity [13] with respect to the modulus technique [9], even in the presence of noise.

2. Model of the system

Many factors causing variations in heart pressure and/or heart rate act on the cardiocirculatory system, thus making it difficult to discern the effects produced by baroreceptors in response to fluctuations in pressure and thus their sensitivity. In order to evaluate measurement problems and explain the proposed technique, the environment in which baroreceptors operate must briefly be described.

Some authors have built up a closed-loop model which considers the possible main factors involved in blood pressure regulation [10,14]. In particular [10], similarly to our study, used the identification method and the PEM but mostly for modelling purposes rather than for measurement.

The overall system is a closed loop (see Fig. 1).

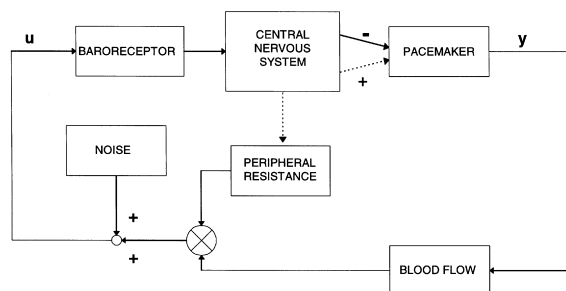


Fig. 1. Diagram of cardiocirculatory and pressure regulation systems. Systolic pressure (mmHg): u ; heart rate (ms): y ; dotted line: effect of vagal system (response time: a few minutes); large circle: multiplication.

Blood pressure, the result of the product of peripheral resistance and cardiac output (Windkessel effect) is measured by the baroreceptors which send a signal to the central nervous system which, by means of sympathetic and vagal reflexes, regulates heart rate through physiological pacemakers. The rate influences heart filling, flow (Starling's law) influences pressure, and so on [14].

This work, by means of linear models, aims at identifying the dynamic behaviour of the chain which has systolic pressure as input 'u' and heart rate as output 'y' (Fig. 1), and at estimating the sensitivity of baroreceptors with pressure variations. Linear models are usually chosen for two main reasons, essentially because of their simplicity, which leads to efficient algorithms for parameter identification, but also because of the lack of knowledge about baroreceptor dynamics which does not justify the adoption of more complicated models.

Many inputs and also noise affect the system. These are:

1. respiration, which causes mechanical compression of the chest, directly influencing blood flow (i.e., it acts as a secondary pump) and thus systolic pressure;
2. tone of peripheral vessels (influenced, for example, by temperature) which directly determines the resistance encountered by blood as it flows;
3. accuracy of non-invasive measurement systems [15,16];
4. baroreceptor sensitivity, influenced by psychological state.

Due to all these effects, correct sensitivity measurements of baroreceptor function become difficult to discern. Analysis of spectral correlation (coherence) [9,13] between pressure and inter-beat interval shows that it may easily fall below 0.5 for various spectral components (see Fig. 2) within the frequency range attributed to baroreceptors: 0.05–0.15 Hz [17].

The modulus method estimates sensitivity by calculating a mean on the harmonics, in the baroreceptor spectral band, which exceed the correlation value of 0.5. The effect of noise is thus reduced.

The method proposed here separates the influence of input from noise by means of parametric identifi-

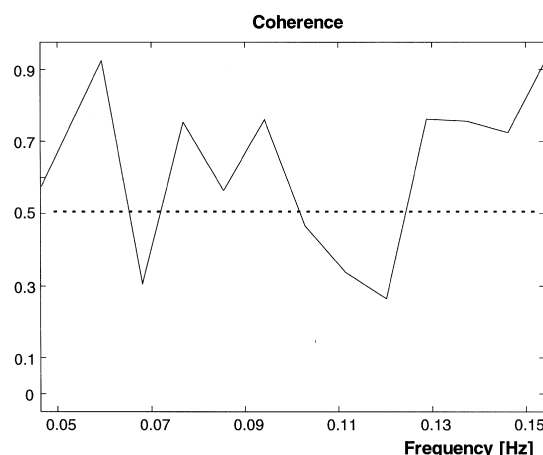


Fig. 2. Example of spectral coherence in 0.05–0.15 Hz baroreceptor band.

cation (ARMAX models whose parameters are obtained by the Prediction Error Method: these models also include noise dynamics). A cost function is defined in the choice of the model, which takes into account not only the sum of square residuals but also the correlation between input and residuals, and auto-correlation of the residuals. In this way, the model which shows the best capacity for representing input–output behaviour is chosen, rather than matching the data only (see Appendix). The estimated sensitivity is the mean on the harmonics of the model transfer-function, computed in the whole baroreceptor band.

3. Experimental data and procedure

Twenty three students participated in a short-duration experimental session. Upon their arrival in the laboratory, and after their informed consent, they were acquainted with the procedure and were prepared for physiological recording. During preparation and recording, subjects were seated in comfortable reclining chairs.

Detection of the R-wave (which was used to build up the heart period sequences) was performed by recording the electrocardiographic signal by Lead II derivation, which enhances R-wave amplitude, and then filtering the signal with a high-pass set to 2 Hz to decrease artifact contamination and slow trends. In

addition, an anti-aliasing filter was set at 200 Hz. The electrocardiogram was sampled with 1ms resolution and stored on a computer. The R-peak was precisely detected by a change in polarity of the first derivative of the cardiac signal. This procedure assures reliable and precise measurement of the time occurrence of the R-wave (within one sample interval, i.e. ± 1 ms). Successive R-wave intervals (IBI = Inter-Beat Interval) were computed with 1 ms precision.

Systolic blood pressure was measured on a beat-to-beat basis by the FINAPRES non-invasive finger plethymographic device (Ohmeda Inc., Louisville, CO). Blood pressure measured by this device has been found to be highly correlated (coherence above 0.8) with pressure recorded intra-arterially [8,15].

FINAPRES necessarily introduces randomly some calibration intervals (lasting 2–4 s) during which the servo-loop of the Finapres adjust the cuff pressure. This data loss was minimized since blood pressure was measured at rest: in such conditions the calibration intervals are few (in average 2 to 4 calibration intervals in 5 min recording). In addition, during calibration intervals blood pressure was

linearly interpolated in order to obtain a contiguous segment of data. However, it is worth noting that the model used here includes these measurement errors as part of the noise characteristics of the system.

During the experimental session two rest sequences of 5 min each were recorded.

The heart does not beat with perfect regularity, consequently systolic pressure and inter-beat interval, recorded at every heart cycle, make up a set of data sampled at irregular intervals. Fig. 3 shows the trend of heart pressure and electrical events as a function of time. The original sequences were interpolated linearly in order to obtain a sequence of 512 samples measured at regular time intervals (sampling interval $T_s = 0.56$ s). Interval $\Delta T(RP)$ between electrical stimulation and pulse wave, was taken into account so as not to introduce delays. The sequences were then filtered by FFT in the 0.05–0.15 Hz band.

4. Identification and model validation

The first rest sequence was divided into two half-sequences of 256 samples each. The identification

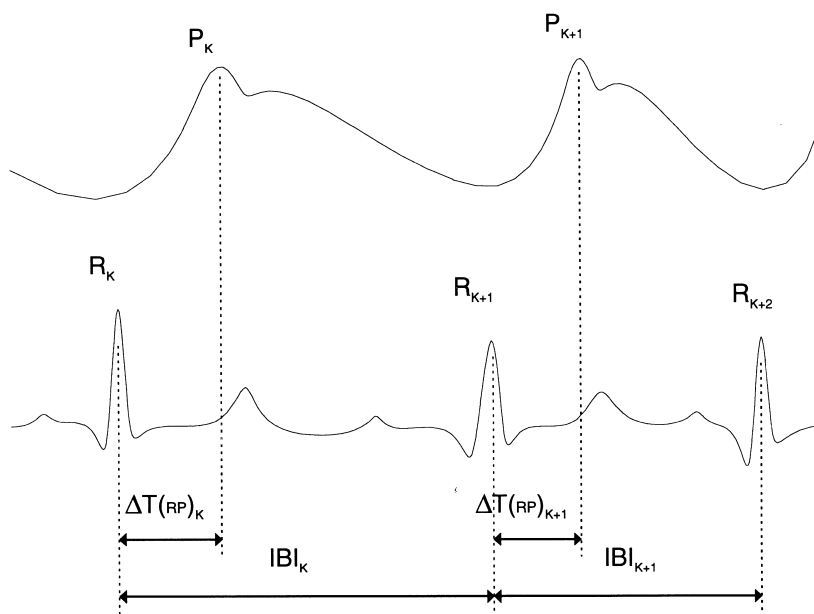


Fig. 3. Qualitative curves representing blood pressure (top) and EKG trace (bottom). Pressure peaks measured with FINAPRES device occur during systole. Lower trace: R-wave interval measures inter-beat period. Note also $\Delta T(RP)$, delay between electrical stimulation and pulse wave.

algorithm was implemented on the first half-sequence, and the model was chosen using the second half-sequence. The second rest sequence was used to validate the identification process and to determine cost function parameters (see Appendix).

The model used here was of the ARMAX type:

$$A(q^{-1})y(t) = B(q^{-1})u(t) + C(q^{-1})e(t)$$

where $u(t)$ is the t -th sample of systolic pressure, $y(t)$ is the t -th sample of inter-beat interval, $A(q^{-1}) = 1 + a_1 \cdot q^{-1} + \dots + a_{n_a} \cdot q^{-n_a}$, q^{-1} is the delay operator: $q^{-1} \cdot y(t) = y(t-1)$, the same is true of $B(q^{-1})$ and $C(q^{-1})$.

Once the order of the model has been fixed by means of n_a , n_b , n_c , and n_k , parameters a_i , b_i and c_i are estimated using the Prediction Error Method, which prevents bias [13].

Poor knowledge of the system does not currently allow hypotheses to be made regarding the order of the model, so that only a higher boundary for the three parameters n_a , n_b and n_c can be established. Once $\Psi = \{n_a, n_b, n_c, n_k / n_i \leq 15; i = a, b, c; n_k = 0\}$, representing the set of all acceptable models, has been defined, together with $\Phi = \{n_a, n_b, n_c, 0 / \Phi \in \Psi\}$, which is the desired model, cost function (Eq. (1)), applied to the whole set, is minimized and thus determines the choice of Φ .

Cost function:

$$A(\lambda, lag) = \sum_{\xi=-lag}^{lag} |C_{ee}(\xi)| + \lambda \cdot \left(\frac{lag}{lag + 10^{-3}} \right) \cdot \sum_{\xi=-lag}^0 |C_{pe}(\xi)| \quad (1)$$

Eq. (1) contains the auto-correlation $C_{ee}(n)$ function of the residuals and the cross-correlation $C_{pe}(n)$ between input (systolic pressure) and residuals. The former embodies two pieces of information: the sum of the square residuals (equal to $C_{ee}(0)$) and the terms of auto-correlation, which indicate to what extent the difference between estimate and experimental values of the inter-beat interval is white noise. The cross-correlation between input and residuals (negative values only) quantifies the correlation between the same signals (the part of sequence $C_{ue}(i > 0)$ indicating feedback is not considered [13]). A high correlation between input and

residuals occurs when the model does not suitably describe the transfer function between input and output. In this case, the non-modelled dynamic remains in the residuals, proportionally raising the correlation. That is, an ideal process of identification involves residuals equal to white noise and completely uncorrelated with input. These considerations led to the definition and application of Eq. (1), in which parameters λ and lag were chosen according to the criteria in the Appendix.

It should also be noted that Eq. (1) is a generalization of the classic least-squares method, i.e.:

$$A(\lambda, 0) = \sum_{t=0}^N e^2(t) \quad (2)$$

where N is the number of samples in the sequences (in our case $N=256$).

Validation was carried out by matching experimental (second rest sequence) and simulated outputs and analysing the normalized cross-correlation between input and residuals [13]:

$$\bar{C}_{pe}(k) \equiv \frac{C_{pe}(k)}{\sqrt{C_{ee}(0) \cdot C_{pp}(0)}} \quad (3)$$

The match between experimental and simulated outputs was acceptable for 90% of subjects. Fig. 4 shows one example of good matching. Correlation between input and residuals (Fig. 5) shows a $k < 0$ trend not exceeding ± 0.3 for all subjects. Instead, for positive out-of-phase values, there was greater

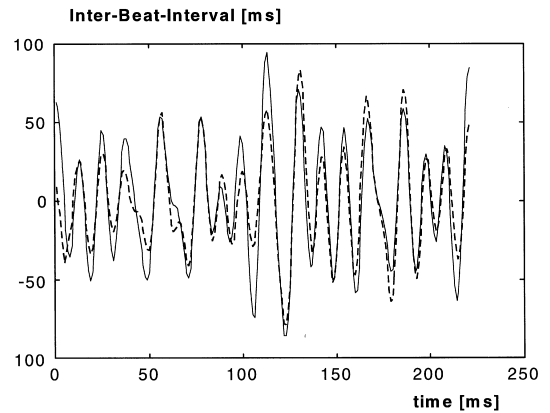


Fig. 4. Example of matching between experimental (dashed line) and simulated values (continuous line).

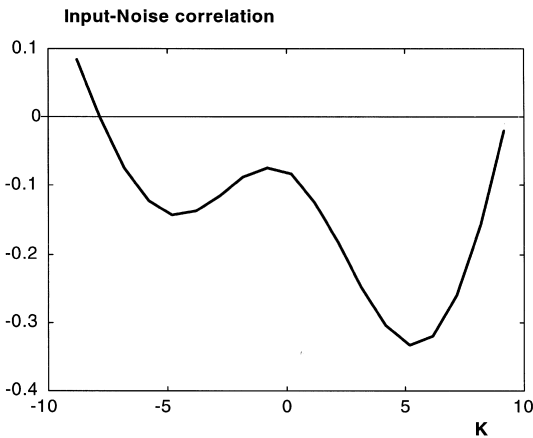


Fig. 5. Normalized cross-correlation between input and residuals.

consistency between input and residuals, since the system is in feedback mode [13].

5. Results

Modulus and identification calibration were carried out by means of simulated data (Fig. 6).

We choose E_K models ($K=1 \dots 46$), resulting from both modelling process: spectral analysis and parametric identification. For each of these models, $N=1 \dots 100$ white noise sequences u were applied as input, with constant root-mean-square values. For

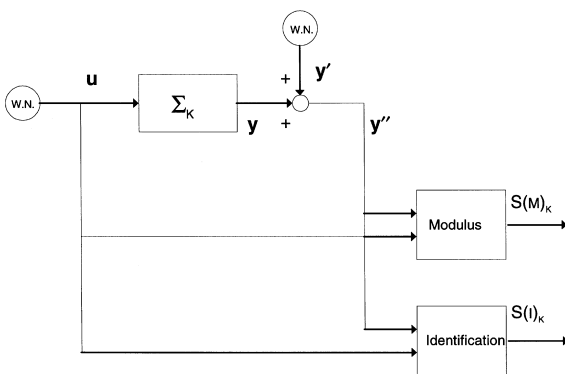


Fig. 6. Calibration of two measurement algorithms by means of simulated data. Forcing input u is white noise; output y is added to noise y' , not correlated with input u , giving virtually measurable output y'' . Couple (u, y'') is supplied to the two algorithms calculating baroreceptor sensitivity.

each of the 100 outputs y , white noise y' was added (independent of forcing noise), giving outputs y'' . Each of the 4600 sequences (u, y'') was processed by the two algorithms which supplied the series of measurements $S(M)_{K,N}$ and $S(I)_{K,N}$ (M =modulus, I =identification).

The true value of sensitivity $S(T)_K$ was defined as the mean of the modulus of the transfer function in the baroreceptor frequency band (ms/mmHg).

The 4600 sequences (u, y'') were used to compare the metrological behaviour of the two algorithms. We computed mean systematic error e_B as a percentage ratio to the true value:

$$e_B(\Psi) \equiv E_K \left\{ \frac{E_N \{ S(\xi)_{K,N} \} - S(T)_K }{S(T)_K} \right\} \cdot 100 \quad (4)$$

and standard deviation of random error e_R :

$$e_R(\Psi) \equiv E_K \left\{ \frac{\sqrt{E_N \{ (S(\xi)_{K,N} - E_N \{ S(\xi)_{K,N} \})^2 \}}}{S(T)_K} \right\} \cdot 100 \quad (5)$$

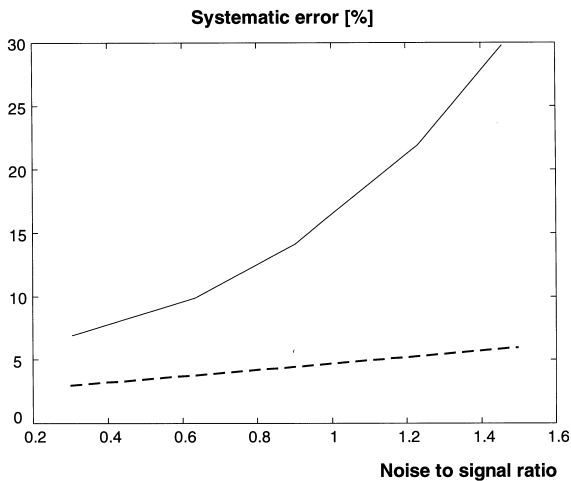
where $E_N(S)$ is the expected value of sensitivity S , for one of the $N=1$ to 100 noise input sequences; $E_K(S)$ is the expected value of sensitivity S , for one of the $K=1$ to 46 resulting models, and Ψ may be the I (Identification) or M (Modulus) method.

The above statistic was repeated for five different values of the ratio between the root-mean-square values of noise y' to output y (see Fig. 7).

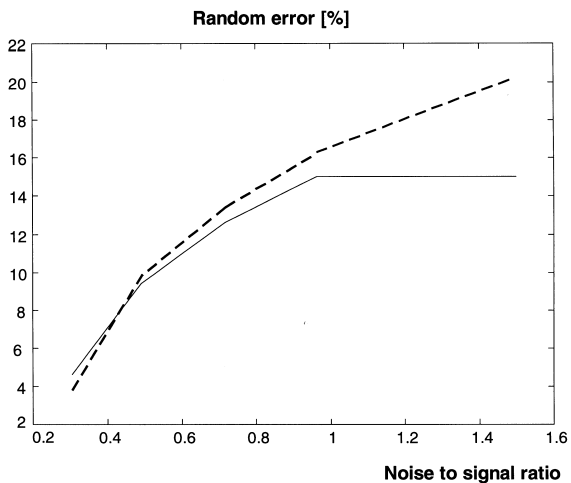
Increasing ratios between noise to signal root-mean-square values, modulus systematic error $e_B(M)$ increased by one order of magnitude with respect to the algorithm proposed here $e_B(I)$. The tendency towards overestimation was 18% (percentage error divided by ratio of noise to signal root-mean-square values). Our technique gave 2.5%. As regards random error, average sensitivities were 11% and 14%, respectively.

The systematic error sensitivity of the modulus technique is due to the incapacity of the algorithm to eliminate the noise components which occur in phase with the signal: these increase spectral consistency instead of reducing it.

The greater robustness of the proposed algorithm lies in the ability of the ARMAX model to identify noise dynamics, decoupling the effect on output by



(a)



(b)

Fig. 7. Trend of Modulus (continuous line) and Identification (dotted line), systematic error e_B (a) and random error e_R (b), as a function of ratio between noise to signal root-mean-square values.

input from that due to measurement errors or interference, and in the choice of cost function.

Random error e_R shows the opposite trend, although to a lesser extent. Possible causes are:

1. the nature of the signals which bring the models to the limit of instability and thus to greater uncertainty in parameter estimation;
2. the new algorithm, being more sophisticated, is more sensitive to measurement error propagation.

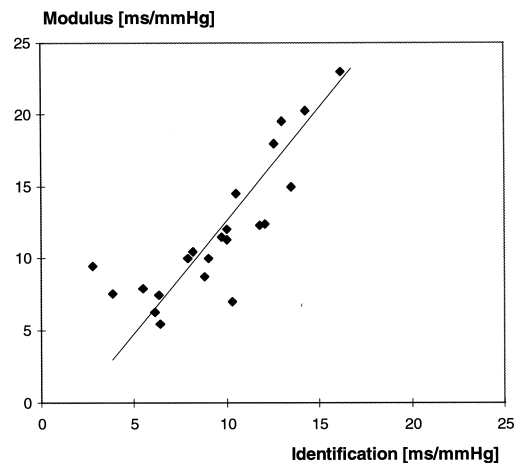


Fig. 8. Comparison between sensitivity measurements using the proposed technique and modulus experimental data.

Taking into account experimental data, regression line $S(M) = \alpha \cdot S(I) + \beta$ between the results of identification and modulus (Fig. 8), gives a correlation of 0.81. As $\alpha = 1.6$ (>1), the modulus tendency to overestimation is confirmed.

6. Conclusions

An alternative technique for calculating the sensitivity of baroreceptors is presented here, exploiting the algorithm of parametric identification of ARMAX models [13].

The new algorithm, modelling the dynamics of output noise, achieves decoupling between desired input and interference. Since in the human vascular system the effects of spurious inputs (respiratory mechanics, vasomotor tone, temperature, etc.) are considerable [10,14], this is a step forward in non-invasive sensitivity measurement techniques.

In the present work, special attention was paid to choosing the ARMAX model with the best characteristics in terms of low correlation between input and residuals. An *ad hoc* cost function was therefore defined, which turned out to demonstrate its efficacy in choosing model order.

The proposed algorithm was compared with a spectral analysis technique named Modulus [9], demonstrating the effectiveness of identification-based techniques [7,11]. Comparison was carried out

by calibrating the two measurement algorithms with simulated data, as a function of increasing noise. Results revealed that modulus tends to overestimate sensitivity, which is not the case with the identification method. The modulus systematic error turned out to be 18% overestimation (percentage error divided by ratio of noise to signal root-mean-square values), whereas with the proposed technique it was only 2.5%.

After checking with simulated data, the two techniques were applied to a set of real data, collected from 23 human subjects at rest. This comparison confirmed the overestimating tendency of the modulus with respect to the identification method.

7. List of symbols

$u(t)$	t -th sample of systolic pressure;
$y(t)$	t -th sample of inter-beat interval;
$A(q^{-1})$	$1 + a_1 \cdot q^{-1} + \dots + a_{n_a} \cdot q^{-n_a}$;
$B(q^{-1})$	$b_1 \cdot q^{-n_k} + \dots + b_{n_b} \cdot q^{-n_b - n_k}$;
$C(q^{-1})$	$1 + c_1 \cdot q^{-1} + \dots + c_{n_c} \cdot q^{-n_c}$;
t	time instant, (sampled at constant rate);
q^{-1}	delay: $q^{-1} \cdot x(t) = x(t-1)$;
$e(t)$	white noise;
$e \equiv T - T'$	are residuals: difference between T (experimental sequence of inter-beat interval) and T' (sequence, estimated by model);
$C_{\xi\eta}(k) = \sum_i \xi(i-k) \cdot \eta(i)$	cross-correlation function between sequences ξ and η ;
$E_\theta\{S\} \equiv (1/n) \sum_{\theta=1}^n S$	expected value of S ;
$\Theta = N$ or K	N is the noise input sequence ($n=100$) and K is the model ($n=46$);
$\Psi = I$ or M	indicates applied method.

Acknowledgements

We are grateful to Prof. F. Angrilli for his helpful comments during the development of the present work.

Appendix 1

This appendix deals with cost-function parameter calculation (lag , λ) and the comparison between the modulus and identification methods. The lag was arbitrarily fixed at 7, in order to cover phase differences between input and residuals of about 75° for the slowest harmonic of the baroreceptor bands: 0.05 Hz. The second rest sequence was divided into two half-sequences of 256 samples each. The first was used to calculate λ and the second for verification purposes. The following were defined: $n(\lambda)$, number of subjects for whom $\text{Re}(\Phi(\lambda, lag)) > \text{Re}(\Phi(\lambda, 0))$; $p(\lambda)$, number of subjects for whom $\text{Re}(\Phi(\lambda, lag)) < \text{Re}(\Phi(\lambda, 0))$; where $\text{Re}(\Phi(\lambda, lag)) = \Lambda(\lambda, 0) |_{\Phi(\lambda, lag)}$ is the sum of square residuals calculated on the first half-sequence for model Φ chosen by function $\Lambda(\lambda, lag)$ applied to the chosen set (second half-sequence of the first recording). In other words, n is the number of subjects for whom matching worsens when the generalised criterion of choice (Eq. (1)) is used with respect to the classic method (least-squares, Eq. (2)). Index p quantifies the number of subjects who show an improvement. A λ value in the interval which minimises index n while maximising p was chosen (see Fig. 9) and was $\lambda \in [1.2 \ 2]$. We calculated the square residuals for the second half-sequence in order to verify cost function parameters: they still came out as $n=0$ and $p=3$. It should also be noted that, in Fig. 9, function $p(\lambda)$ is always greater than $n(\lambda)$, indicating that there is always a

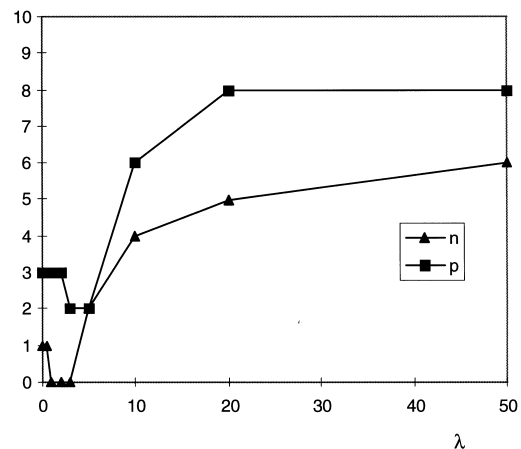


Fig. 9. Trend of functions $n(\lambda)$ and $p(\lambda)$ according to parameter λ .

higher number of subjects who show improvement. As further validation of the method, the phase trend for models chosen using the new criterion (Eq. (1)) and the classic least-squares method (Eq. (2)) was verified. The number of models which differ out of a total of 23 subjects, because of the two different criteria of choice, were four (for one of whom no significant difference in residuals was found). Two subjects showed a positive phase trend when the classic criterion was chosen, but negative when the new criterion was used (Fig. 10). This is further confirmation of the validity of the criterion used

here, which allows leading-phase models (i.e., those contrary to the principle of cause-effect) to be discarded.

References

- [1] M. Kessler, R. Pietrosky, Baroreceptor sensitivity and hypertension, in: T. Elbert, W. Langosh, A. Steptoe, D. Vaitl Behavioural Medicine in Cardiovascular Disorders, Wiley, New York, 1988, pp. 5–16.
- [2] T. Elbert, B.R. Dworkin, H. Rau, et al., Sensory effects of baroreceptor activation and perceived stress together predict long-term blood pressure elevation, *Int. J. Behav. Med.* 1 (1994) 215–228.
- [3] A. Takeshita, S. Tanaka, A. Kuroiwa, M. Nakamura, Reduced baroreceptor sensitivity in borderline hypertension, *Circulation* 51 (1975) 738–742.
- [4] G. Parati, M. Di Rienzo, G. Bertinieri, et al., Evaluation of the baroreceptor-heart rate reflex by 24-hour intra-arterial blood pressure monitoring in humans, *Hypertension* 12 (1988) 214–222.
- [5] G.E. Billman, P.J. Schwartz, H.L. Stone, Baroreceptor reflex control of heart rate: a predictor of sudden cardiac death, *Circulation* 66 (1982) 874–880.
- [6] H.S. Smyth, P. Sleight, G.W. Pickering, Reflex regulation of arterial pressure during sleep in man: a quantitative method of assessing baroreflex sensitivity, *Circ. Res.* 24 (1969) 109–121.
- [7] M. Pagani, V. Somers, R. Furlan, et al., Changes in autonomic regulation induced by physical training in mild hypertension, *Hypertension* 12 (1988) 600–610.
- [8] S. Omboni, G. Parati, A. Frattola, et al., Spectral and sequence analysis of finger blood pressure variability. Comparison with analysis of intra-arterial recordings, *Hypertension* 22 (1993) 26–33.
- [9] H.W.J. Robbe, L.J.M. Mulder, H. Rüddel, W.A. Langewitz, J.B.P. Veldman, G. Mulder, Assessment of baroreceptor reflex sensitivity by means of spectral analysis, *Hypertension* 10(5) (1987) 538–542.
- [10] G. Baselli, S. Cerutti, F. Badilini, Model for the assessment of heart period and arterial pressure variability interactions and of respiration influences, *Med. Biol. Eng. Comput.* 32 (1994) 143–152.
- [11] D.J. Patton, J.K. Friedman, M.H. Perrot, A.A. Vidian, J.P. Saul, Baroreflex gain: characterization using autoregressive moving average analysis, *Am. J. Physiol.* 270 (1997) H1240–H1249.
- [12] A. Malliani, M. Pagani, F. Lombardi, F. Cerutti, Cardiovascular neural regulation explored in the frequency domain, *Circulation* 84 (1991) 482–492.
- [13] T. Söderström, P. Stoica (Eds.), *System Identification*, Prentice Hall, 1989.
- [14] R.W. De Boer, M. Karemaker, J. Strackee, Hemodynamic fluctuations and baroreflex sensitivity in humans: a beat to beat model, *Am. J. Physiol.* 253 (1987) 680–689.

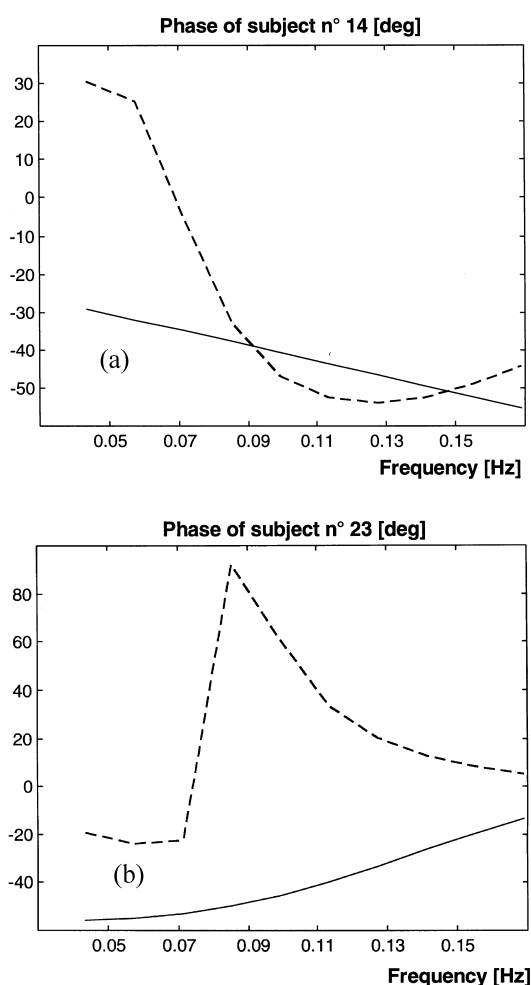


Fig. 10. Phase of transfer function of model chosen using equations (2) (dotted line) and (1) (continuous line). Analyses were performed over typical baroreceptor frequency range (0.05–0.15 Hz).

- [15] T. Kurky, N.T. Smith, N. Head, H. Dee-Silver, A. Quinn, Non-invasive continuous blood pressure measurement from the finger: optimal measurement conditions and factors affecting reliability, *J. Clin. Monit.* 3 (1987) 6–13.
- [16] K.H. Wesseling, J.J. Settels, G.M.A. VanDerHoeven, J.A. Nijboer, M.W.T. Butuin, J.C. Dorlas, Effects of peripheral vasoconstriction on the measure of blood pressure in a finger, *Cardiovasc. Res.* 19 (1985) 139–145.
- [17] M. Pagani, O. Rimoldi, M.R. Pagani, Sympathetic afferents and neural control of the circulation, in: D. Vaitl, R. Shandry (Eds.), *From the Heart to the Brain: the Psychophysiology of Circulation-Brain Interaction*, Peter Lang GmbH, Frankfurt, 1995, pp. 61–81.